

# Effects of Zn Addition on Microstructure and Mechanical Properties of Mg-8Al-2Sn Alloy

Wu Huayi<sup>1</sup>, Zhang Dingfei<sup>1</sup>, Jiang Luyao<sup>1</sup>, Feng Jingkai<sup>1</sup>, Zhao Yang<sup>1</sup>,  
Pan Fusheng<sup>2</sup>

<sup>1</sup> National Engineering Research Center for Magnesium Alloys, Chongqing University, Chongqing 400044, China; <sup>2</sup> Chongqing Academy of Science and Technology, Chongqing 401123, China

**Abstract:** The effect of adding 0 wt%–2.0 wt% Zn to Mg-8Al-2Sn alloy was investigated by analyzing the microstructures and tensile properties. The results reveal that the phase composition of Mg-8Al-2Sn-*X*Zn alloys is  $\alpha$ -Mg, Mg<sub>17</sub>Al<sub>12</sub> and Mg<sub>2</sub>Sn phases. The morphology of eutectic phase of the as-cast alloys with Zn addition changes from a normal eutectic structure to a divorced eutectic structure. Grain sizes of the alloys with Zn addition are uniform after hot extrusion. Dynamic precipitation of the second phases is promoted by the addition of Zn during hot extrusion. The second phases are coarsened in Mg-8Al-2Sn-2Zn alloy. Precipitates form during the aging treatment and their amount increases with the addition of Zn. Besides, the ultimate tensile and yield strength of the extruded and aged alloys gradually increase with the addition of Zn. Mg-8Al-2Sn-2Zn alloy has the best mechanical property, and the ultimate tensile strength, yield strength and elongation of the as-aged alloy are 385 MPa, 291 MPa and 6.44%, respectively.

**Key words:** magnesium alloys; Mg-Al-Sn-Zn alloy; extrusion; microstructure; mechanical properties

As magnesium (Mg) alloys are the lightest structural metals currently available, they have received steadily increasing attention in the transportation industry and electronics industry because of high specific strength, high stiffness, high thermal conductivity, good electromagnetic shielding characteristics, and superior damping capacity. In particular, magnesium (Mg) alloys can provide large weight savings compared to conventional aluminum alloys, so they are particularly attractive for transportation vehicles and aerospace applications<sup>[1-6]</sup>. The worldwide emphasis on increasing fuel efficiency in automobiles has thrust magnesium alloys into the fore as potentially lightweight materials for structural applications. It is believed that this trend in light weighting automobiles will continue, and if suitable magnesium alloys can be developed, they will replace heavier aluminum and steel based counterparts. Wrought Mg alloys offer better mechanical properties than cast Mg alloys because of the pronounced grain refinement,

non-pores and uniform composition distribution after the deformation process.

At present, Mg-Al series alloys, as the most commonly used magnesium alloys, display excellent cast ability and low cost. However, the large scale application of these alloys is restricted by their insufficient strength. Further improvement in the strength of these alloys is needed to expand their use to a wider range, as their current maximum strength is still less than that of commercial high-strength Al alloys which often represent a major competition to Mg alloys. Adding trace strengthening elements to the alloys is considered an important approach to improve the properties. The addition of diverse elements can form different precipitates and modify the mechanical properties of alloys. Sn is a metal element with a low melting point which is easily added during the process of smelting magnesium alloy. In addition, the Mg-Sn system is a good candidate for precipitation hardening because of the

Received date: July 12, 2018

Foundation item: National Great Theoretic Research Project (2013CB632200); National Natural Science Foundation of China (51571040, 51531002); National Great Engineering Research Project (2016YFB0301101)

Corresponding author: Zhang Dingfei, Ph. D., Professor, College of Materials Science and Engineering, Chongqing University, Chongqing 400044, P. R. China, Tel: 0086-23-65112491, E-mail: zhangdingfei@cqu.edu.cn

Copyright © 2019, Northwest Institute for Nonferrous Metal Research. Published by Science Press. All rights reserved.

large difference in solid solubility in Mg at high temperature (3.35 at% at 561 °C) and low temperature (0.035 at% at room temperature). The phase diagram of the Mg<sub>2</sub>Sn system shows the formation of an equilibrium stable phase of Mg<sub>2</sub>Sn with an fcc structure<sup>[7]</sup> and a high melting point of 770 °C. The high temperature stability for the Mg<sub>2</sub>Sn phase gives the alloys based on Mg-Sn huge potential to be used in higher temperature creep resistant applications<sup>[8,9]</sup>. The research<sup>[10]</sup> showed that the comprehensive mechanical properties of magnesium alloy can be obviously improved with the addition of Sn. Avraham et al<sup>[11]</sup> also studied the effect of Sn on the microstructure and properties of the Mg-Al alloy. It was found that the mechanical properties of the alloy can be improved by forming the finely dispersed Mg<sub>2</sub>Sn phase in the crystal or reducing the formation of Mg<sub>17</sub>Al<sub>12</sub> phase<sup>[12]</sup>. And stacking fault energies of Mg-Al based alloys can be reduced by the presence of Sn and the ductility of the alloys is improved<sup>[13]</sup>. Based on previous researches, Mg-Al-Sn alloys are being developed as a new series of Mg alloys. Besides this, the main function of Mn is to purify the melt. Since it is inevitable to introduce Fe, which is harmful to the corrosion properties, into Mg alloys during the smelting process, Mn and Fe can form MgFeMn compounds which can be settled in the process of smelting. So a certain amount of Mn is usually added into Mg alloys to remove the Fe element.

In 2004, Bowles<sup>[14]</sup> investigated the microstructure of the Mg-Sn alloys and the Mg-Al-Sn alloys. The results showed that there are  $\alpha$ -Mg, Mg<sub>2</sub>Sn and Mg<sub>17</sub>Al<sub>12</sub> phase in Mg-Al-Sn alloys, and no ternary phase exists. In 2007, Doernber et al<sup>[15]</sup> also investigated the Mg-Al-Sn ternary alloy and pointed out that there is no ternary phase, and the third element has no solid solubility in the binary phase. The R&D team for materials research of Japan National Institute has been working on the Mg-Sn alloy since 2000. In 2006, Sasaki and Mendis et al<sup>[10,16]</sup> found that the addition of Zn can change the morphology, volume fraction and phase relation of precipitated phases of Mg-Sn alloy. And the aging strengthening ability of the Mg-Sn alloy can be improved significantly with the addition of Zn<sup>[17]</sup>. Through the characterization of the microstructure by TEM, it was found that a large amount of Mg<sub>2</sub>Sn precipitate is formed along the <0001> direction in the crystal, indicating that the addition of a certain amount of Zn can promote the formation of Mg<sub>2</sub>Sn phase in the alloy. Mg<sub>2</sub>Sn phase can improve the second phase strengthening. Moreover, the increase of Mg<sub>2</sub>Sn can improve the high temperature property of magnesium alloy because of the high melting point of Mg<sub>2</sub>Sn phase<sup>[18,19]</sup>. The researches displayed that Zn is a major addition element because it has potential to develop the mechanical properties in Mg-Al-Sn systems<sup>[20]</sup>.

Despite the above findings, there is still a lack of optimization of Zn content for the Mg-8Al-2Sn alloy. Therefore, the purpose of this work is to better understand the effect of Zn on the microstructure and mechanical properties of the

Mg-8Al-2Sn alloy, and to determine the optimal composition of the Mg-8Al-2Sn-XZn alloys (X=0.0~2.0, wt%).

## 1 Experiment

The nominal composition of the alloy studied was Mg-8Al-2Sn-XZn (X=0, 0.5, 1.0 and 2.0, wt%) based on AT82, AZT802, AZT812, AZT822. To prepare billets for extrusion, alloys with different composition were melted under a vacuum atmosphere of Ar, and then stabilized at 740 °C. After holding each melt at 740 °C for 20 min, they were poured into a steel mold and then pre-heated to 200 °C. The composition of each billet was measured using X-ray fluorescence (XRF) and found to be very close to their nominal values, given in Table 1. Homogenization was then conducted at 420 °C for 12 h, less than the calculated melting temperature of each alloy. Extrusion experiments were carried out at an initial billet temperature of 380 °C, a punching speed of 1 m/min, and an extrusion ratio of 25. The capacity of the horizontal extruder used was 500 t, and the diameter of the extrusion barrel was 80 mm.

The alloy specimens were then subjected to a subsequent aging treatment at 175 °C for different time up to 20 h (T5) in order to determine the appropriate heat treatment time for the alloys. The aging-hardening response was determined by a micro Vickers hardness tester under a load of 50 g for 60 s, and hardness values obtained by ten indentations were averaged for each hardness value reported here.

The microstructure of each alloy was observed using optical microscopy (OM), scanning electron microscopy (SEM), energy dispersive spectrometer (EDS), X-ray diffraction analysis (XRD). The longitudinal tensile properties of the as-extruded alloys and the aged alloys were measured at room temperature with an initial strain rate of  $1.43 \times 10^{-3} \text{ s}^{-1}$ . Dogbone-shaped specimens with a gage length of 35 mm and a gage diameter of 5 mm were used for the tensile tests.

## 2 Results and Discussion

### 2.1 Phase diagram analysis

The phase diagram analysis and calculation of Mg-8Al-2Sn-0.3Mn-XZn alloy were made by Pandat. And the composition was Al 8.5 wt%, Sn 2 wt%, Mn 0.3 wt%, and Zn 0 wt%~5.0 wt%. As shown in Fig.1, a small increase of the liquidus temperature and an obvious change of the solidus temperature can be seen. When the Zn content increases from 0 wt% to 1.99 wt%, the solidus temperature decreases from 483 °C to 396 °C.

**Table 1** Actual composition of AT82-XZn alloys (wt%)

Alloy	Mg	Al	Sn	Mn	Zn
AZ82	89.07	8.11	2.69	0.13	0
AZT802	88.33	8.38	2.50	0.16	0.63
AZT812	87.71	8.57	2.46	0.15	1.11
AZT822	86.88	8.31	2.42	0.14	2.25

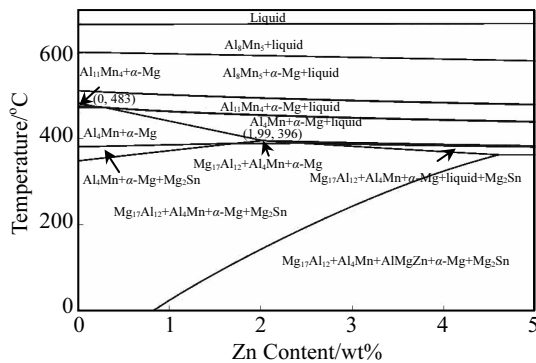


Fig.1 Phase diagram of Mg-8Al-2Sn-0.3Mn-XZn alloy

The effect of the Al-Mn phase can be ignored because of the content of Mn. It can be considered that a single phase solid solution of  $\alpha$ -Mg forms in the range of 0 wt%~1.99 wt% Zn. When the Zn content is higher than 1.99 wt%, the alloy is mainly composed of  $\alpha$ -Mg and  $Mg_{17}Al_{12}$  phase. If the content of Zn is too high, the single phase solid solution cannot be obtained. Therefore, the Zn content of the alloy was 0 wt%~2.0 wt% in this study.

## 2.2 As-cast microstructures

The optical micrographs of the as-cast AT82 alloy with various Zn contents are shown in Fig.2. It can be found that the microstructure of as-cast AT82-XZn alloy consists of pri-

mary  $\alpha$ -Mg matrix and eutectic compounds at the grain boundary. As shown in Fig.2, with the addition of Zn, the number of the second phases and the volume fraction of eutectic compounds at grain boundaries increase.

XRD patterns of as-cast AT82-XZn alloys are shown in Fig.3. It is confirmed that the microstructure of the as-cast alloys consists of  $\alpha$ -Mg,  $Mg_{17}Al_{12}$ , and  $Mg_2Sn$  phases. To determine the formation of new phases, SEM and EDS analyses of AT82-XZn alloys were carried out, as shown in Fig.4 and Table 2, respectively. Combining the EDS (Table 2) analysis with the XRD pattern (Fig.3), it can be determined that the main composition of as-cast alloys is  $\alpha$ -Mg phases,  $Mg_2Sn$  phases and  $Mg_{17}Al_{12}$  phases.

The EDS and SEM analyses of as-cast AT82-XZn alloys indicate that the microstructure of the as-cast alloy has the eutectic characteristic, and is mainly composed of compounds with gray contrast and bright white contrast. And the gray phase at the grain boundary of area A in Fig.4c is  $Mg_{17}Al_{12}$  phase. The bright phase of area B in Fig.4c also at the grain boundary is  $Mg_2Sn$  phase. The bright phase which is the same as the area C in Fig.4d is Al-Mn phase. Furthermore, from the morphology and distribution of the eutectics in the as-cast alloys in Fig.4, it can be clearly seen that the equilibrium eutectic structure is distributed at grain boundaries in the as-cast AT82 alloy, as shown in Fig.4a. With the addition of Zn, the eutectic microstructure in the as-cast AZT802, AZT812 and AZT822 alloys shows the divorced eutectic morphology, as shown

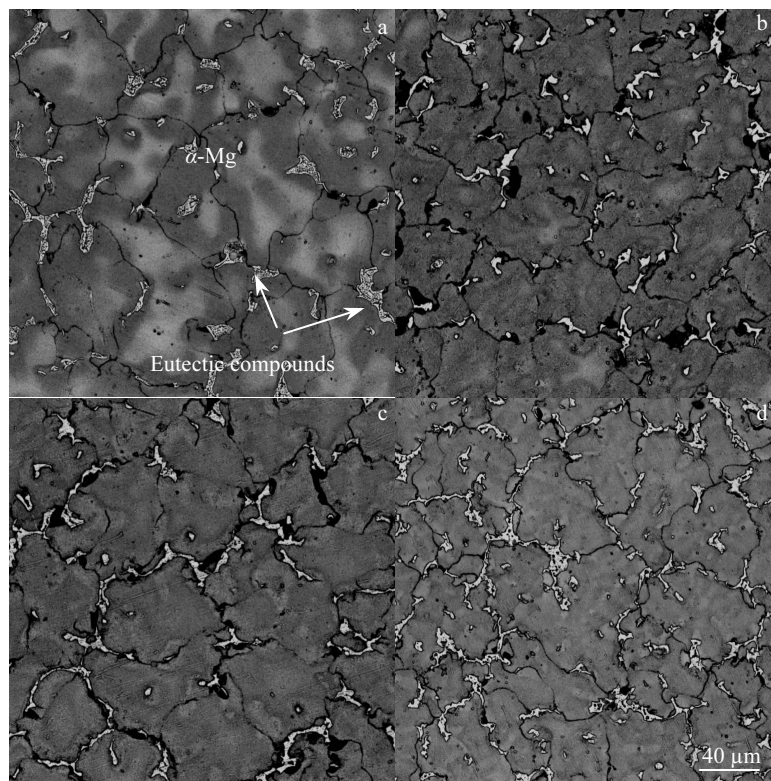


Fig.2 Optical microstructures of as-cast AT82 (a), AZT802 (b), AZT812 (c), and AZT822 (d)

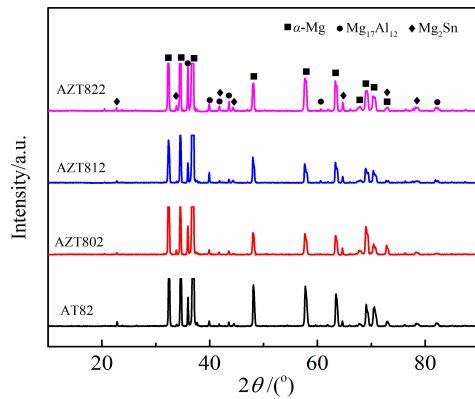


Fig.3 XRD patterns of as-cast AT82-*X*Zn alloys

in Fig.4b–4d. The combination of the EDS (Table 2) analysis and the XRD pattern (Fig.3) can confirm that the phases with divorced eutectic structure presenting block and strip are  $Mg_{17}Al_{12}$  phases. Moreover, with the Zn addition, the aggregation of  $Mg_2Sn$  phases can be promoted. It can be found that the morphology of  $Mg_2Sn$  phase changes from fine to blocky.

### 2.3 As-extruded microstructures

The optical microstructures of as-extruded AT82-*X*Zn ( $X=0, 0.5, 1, 2, \text{wt}\%$ ) alloys in Fig.5, in which the direction of view is perpendicular to the direction of extrusion, reveal that the grain of the extruded alloy is obviously refined, because dynamic recrystallization occurs during the extrusion deformation. Moreover, there is an obvious extrusion streamline along extrusion direction, as shown in Fig.5. It also can be seen that many fine grains are distributed at the streamline and larger grains are distributed between streamlines. This seems to be

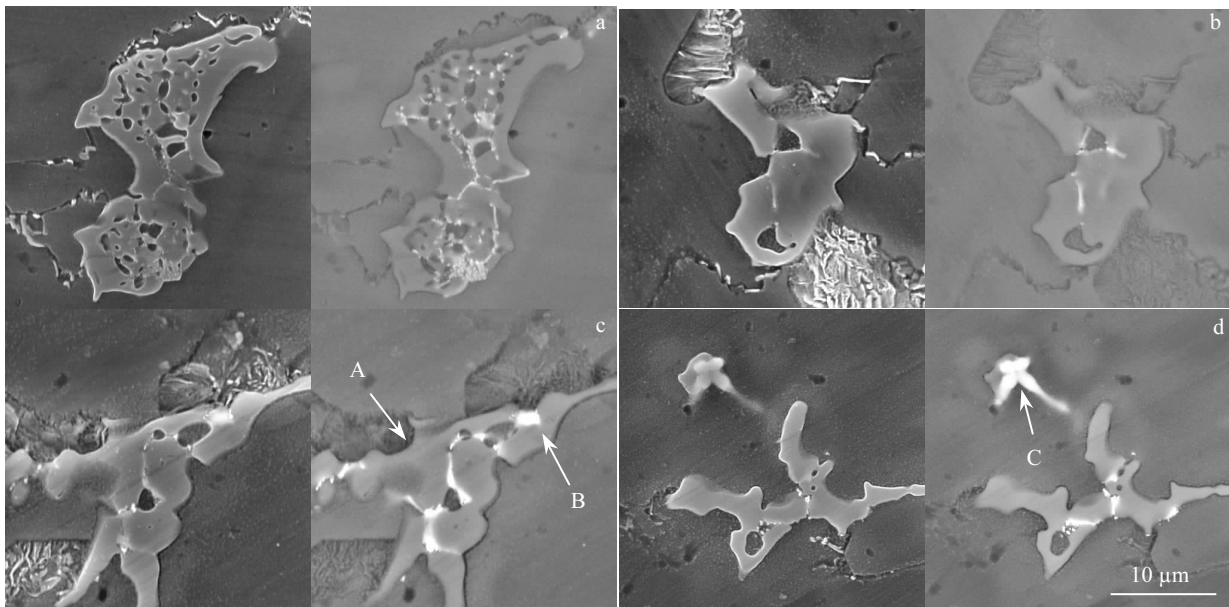


Fig.4 SEM microstructures of as-cast AT82 (a), AZT802 (b), AZT812 (c), and AZT822 (d)

**Table 2** EDS analysis of areas A, B and C in Fig.4 (wt%)

Area	Mg	Al	Sn	Zn	Mn	Fe
A	64.68	27.14	4.36	3.82	0	0
B	64.02	15.52	18.36	2.08	0	0
C	32.86	39.63	0	0.14	25.62	1.89

responsible for the fact that more second phases are distributed at the streamlines which can effectively pin the movement of dislocation during hot extrusion, and also have significant grain refinement effect. Besides, it is obvious that the microstructure uniformity of alloys is improved with Zn addition after hot extrusion. Particularly, in the extruded AZT812 alloy, its microstructure is very uniform.

It can be more clearly seen from the SEM image in Fig.6a

that there are fine grain zone and coarse grain zone in AT82 due to the distribution of the second phase. This is because the second phases can pin the movement of dislocation and have significant grain refinement effect. The directional distribution of the second phase particles in the extruded alloy under compressive stress results in an extrusion streamline along the extrusion direction. In addition, with the increase of Zn content, it is observed that the number and size of the second phase in the extruded alloy also increase. The second phases are coarsened in the AZT822 alloy. Therefore, it is inferred that dynamic precipitation of the second phases is promoted by the addition of Zn during hot extrusion.

### 2.4 As-aged microstructures

The hardness curves of the alloys aged at uniform temperature are presented in Fig.7. It can be seen that the hardness is

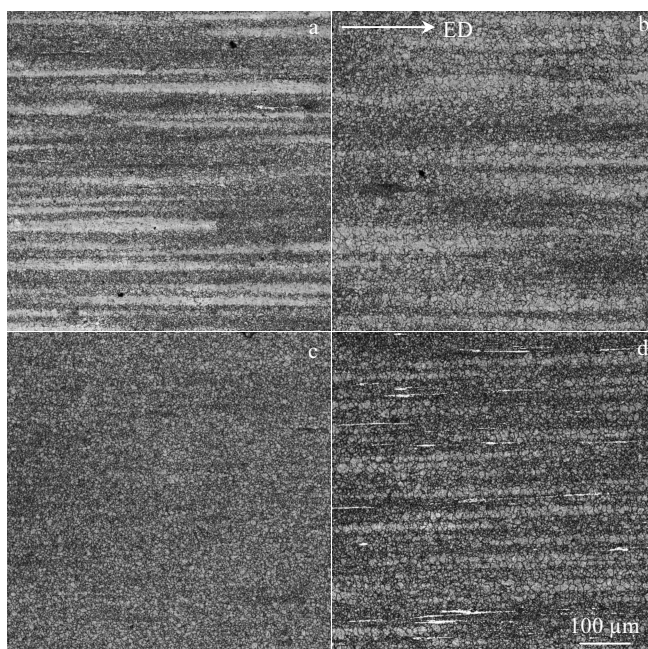


Fig.5 Optical microstructures of as-extruded AT82 (a), AZT802 (b), AZT812 (c), and AZT822 (d)

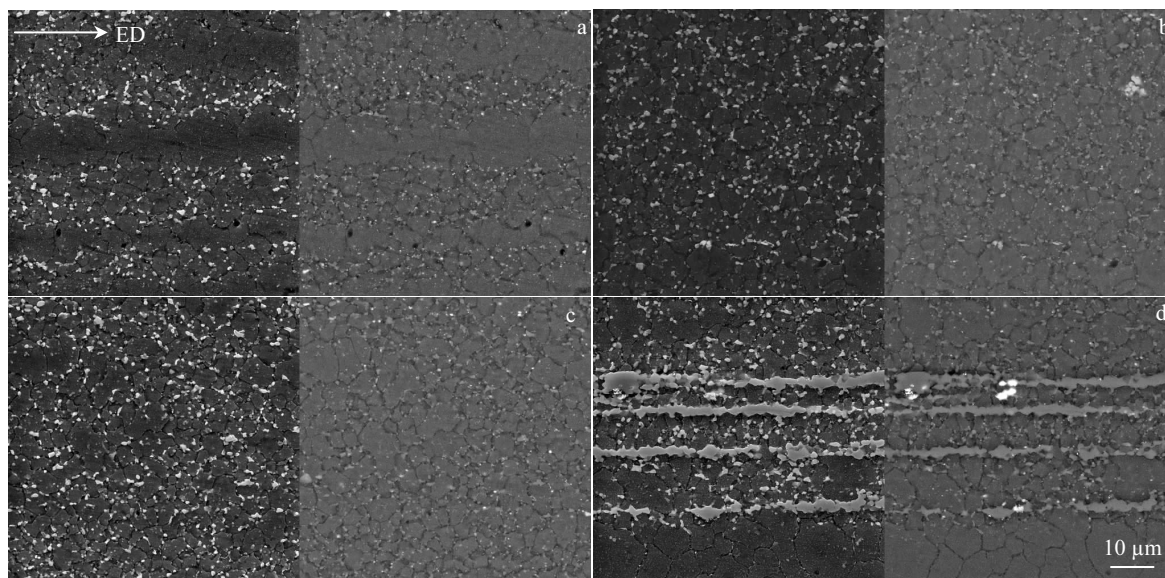


Fig.6 SEM microstructures of as-extruded AT82 (a), AZT802 (b), AZT812 (c), and AZT822 (d)

obviously improved with the addition of Zn. Furthermore, the hardness of the four alloys increases to a peak and then decreases gradually. The increase of hardness is due to the new precipitate formed during aging treatment, which exerts an effect of dispersion strengthening. The hardness gradually tends to a steady value after 3 h, because the precipitated phase has reached the saturation state. After the alloy reaches the hardness peak (peak-aging), overaging occurs. It can be observed that the peak-aging time of AT82 and AZT802 alloys is 3 h, and that of

AZT812 and AZT822 alloys is 5 h. Thus, the addition of Zn can delay the aging hardening peak. And the aging process of AT82 and AZT802 alloy is determined to be 175 °C/3 h, and that of AZT812 and AZT822 is 175 °C/5 h.

SEM images for the alloys in the peak age hardening stage are shown in Fig.8. It can be observed that the gray phase in the alloy is  $Mg_{17}Al_{12}$  phase, and the bright phase is  $Mg_2Sn$  phase. In addition, with the increase of Zn content, the number of the  $Mg_2Sn$  phase and the size of the second phases in the alloy both

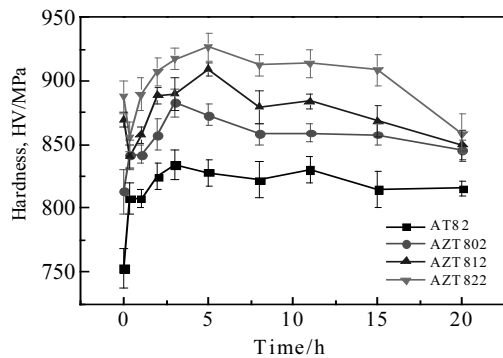


Fig.7 Hardness curves of the AT82-XZn alloys aged at 175 °C

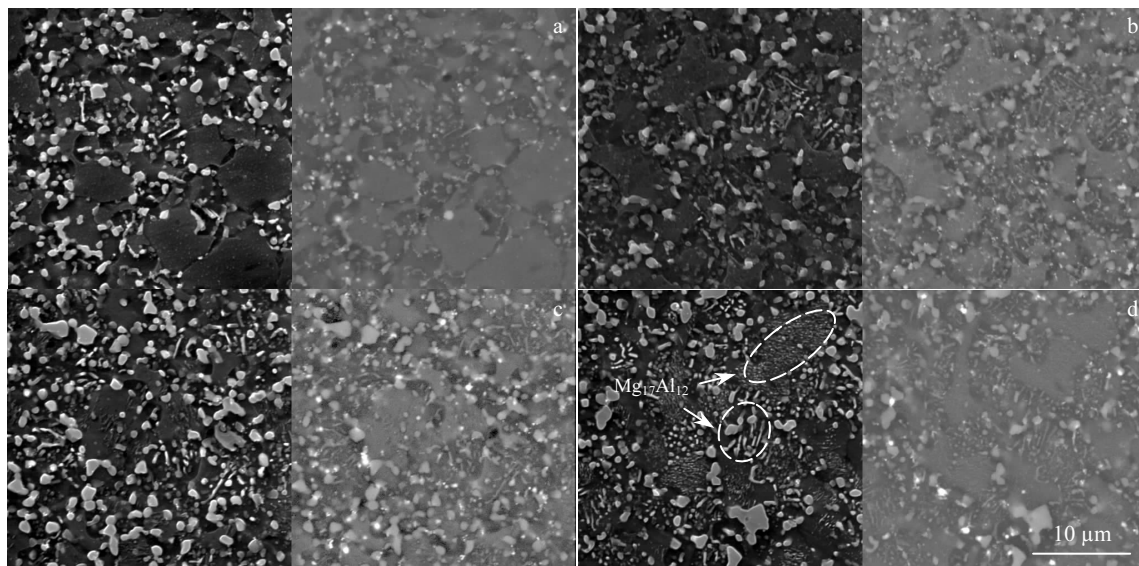


Fig.8 SEM microstructures of as-aged AT82 (a), AZT802 (b), AZT812 (c), and AZT822 (d)

increase of Zn content. However, the elongation of the alloy decreases slightly with the increase of strength. When the content of Zn is 2 wt%, the combination properties of the as-extruded and as-aged alloys both reach an optimum, in which the YS, UTS and EL are increased to 258 MPa, 357 MPa and 8.76% for the as-extruded alloy, and 291 MPa, 385 MPa and 6.44% for the as-aged alloy, respectively.

For the extruded alloy, the yield strength and ultimate tensile strength of AZT802 are less than those of AT82. The reason is that there are fine grain zone and coarse grain zone in AT82 alloy, where the deformation of soft matrix and hard matrix in the mixed crystal structure can enhance the strength. Wu et al.<sup>[23]</sup> investigated the back-stress strengthening of the mixed crystal structure on titanium alloys. The results show that the Bauschinger effect of the mixed crystal attributes to strengthening ability. Moreover, as mentioned above, an obvious increase of the amount of the second phase is observed in the alloy with the increase of Zn content after hot extrusion, which can exert the effect of dispersion strengthening. Thus, the mechanical properties of the alloys are improved with the increase of the second

increase. It also can be found that precipitates form during the aging treatment and their amount increases with the addition of Zn content. As shown in Fig.8d, in terms of morphology, the typical precipitates are  $Mg_{17}Al_{12}$ <sup>[21,22]</sup>, including large lamellar discontinuous precipitates and thin lamellar continuous precipitates.

## 2.5 Mechanical properties

The stress-strain curves of the as-extruded and as-aged AT82-XZn alloys are shown in Fig.9, and the tensile properties of the as-extruded and as-aged AT82-XZn alloys including yield strength (YS), ultimate tensile strength (UTS) and elongation (EL) are listed in Table 3. It is shown that the ultimate tensile and yield strength of the alloys are gradually enhanced with the

phase. It can be found that the strength of AZT812 and AZT822 are improved prominently, as shown in Fig.9 and Table 3. Although the size of the second phase also increases due to the addition of Zn, the changes in the size have little effect on the mechanical properties. Dispersion strengthening plays a major

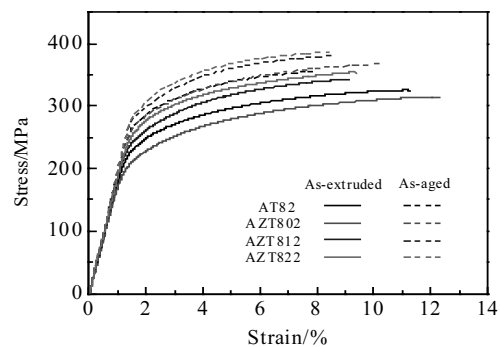


Fig.9 Stress-strain curves of the as-extruded and as-aged AT82-XZn alloys

**Table 3 Mechanical properties of as-extruded and as-aged alloys**

Alloy	As-extruded			As-aged		
	YS/MPa	UTS/MPa	EL/%	YS/MPa	UTS/MPa	EL/%
AZ82	226	326	9.54	265	357	8.40
AZT802	201	311	10.6	268	365	8.76
AZT812	251	354	8.06	280	378	7.00
AZT822	258	357	8.76	291	385	6.44

role in the range of 2 wt%. For the aged alloy, it is well known that second phase strengthening is generally beneficial to the tensile properties of the alloys. With the addition of Zn, the amount of precipitated phases in the aged alloy also increases, which have a second phase strengthening effect on the alloy. Thus, the mechanical properties are enhanced. Furthermore, the disparity of as-extruded and as-aged alloys shows that the mechanical properties of the aged alloy are better than those of the extruded alloy. The strength of the alloy is further improved owing to the formation of precipitated phases during aging treatment, which plays a role in the second phase strengthening.

### 3 Conclusions

1) The phase composition of as-cast AT82-*X*Zn alloys is  $\alpha$ -Mg, Mg<sub>17</sub>Al<sub>12</sub> and Mg<sub>2</sub>Sn phases. And the morphology of eutectic phases of the as-cast alloy changes from a normal eutectic structure to a divorced eutectic structure with the addition of Zn. In addition, with the increase of Zn content, the aggregation of Mg<sub>2</sub>Sn phases can be promoted.

2) After extrusion deformation, the grain size is refined significantly. Moreover, an obvious extrusion streamline along extrusion direction is observed in extruded AT82-*X*Zn alloys. And there are fine grain zone and coarse grain zone in the alloys because of the distribution of the second phases. Additionally, the microstructure uniformity of alloys is improved with the addition of Zn after hot extrusion. Dynamic precipitation of the second phases is also promoted by the addition of Zn during the hot extrusion process. And the second phases in AZT822 alloy are coarsened.

3) At the aging temperature of 175 °C, the aging time of AT82 and AZT802 alloy is determined to be 3 h, and that of AZT812 and AZT822 is determined to be 5 h. The addition of Zn can delay the aging hardening peak. Furthermore, precipitates form during the aging treatment and their amount increases with the addition of Zn.

4) The ultimate tensile and yield strength of the extruded and aged alloys gradually increase with the addition of Zn. Mg-8Al-2Sn-2Zn alloy has the best mechanical property, and the ultimate tensile strength, yield strength and elongation of the as-aged alloy are 385 MPa, 291 MPa and 6.44%, respectively.

### References

- Polmear I J. *Materials Science and Technology*[J], 1994, 10(1): 12
- Liu Juan, Cui Zhenshan. *Journal of Materials Processing Technology*[J], 2009, 209 (18-19): 5871
- Friedrich H, Schumann S. *Journal of Materials Processing Technology*[J], 2001, 117(3): 276
- Mordike B L, Ebert T. *Materials Science and Engineering A*[J], 2001, 302(1): 37
- Cao Z, Wang F H, Wan Q et al. *Materials & Design*[J], 2015, 67: 64
- Wang L F, Mostaed E, Cao X Q et al. *Materials & Design*[J], 2016, 89: 1
- Nayeb-Hashemi A A, Clark J B. *Bulletin of Alloy Phase Diagrams*[J], 1984, 5(5): 466
- Bowles A L, Dieringa H, Blawert C et al. *Materials Science Forum* [J], 2005, 488-489: 135
- Sasaki T T, Oh-Ishi K, Ohkubo T et al. *Materials Science & Engineering A*[J], 2011, 530(12): 1
- Sasaki T T, Oh-ishi K, Ohkubo T et al. *Scripta Materialia*[J], 2006, 55(3): 251
- Avraham S, Katsman A, Bamberger M. *Proceedings of Magnesium Technology*[C]. Seattle: TMS, 2010: 377
- Son H T, Lee J B, Jeong H G et al. *Materials Letters*[J], 2011, 65(12): 1966
- Wang H Y, Zhang N, Wang C et al. *Scripta Materialia*[J], 2011, 65(8): 723
- Bowles L, Blawert C, Norbert H et al. *Magnesium Technology*[J], 2004: 307
- Doernber G E, Kozlov A, Schmid-Fetzer R. *Journal of Phase Equilibria & Diffusion*[J], 2007, 28(6): 523
- Mendis C L, Bettles C J, Gibson M A et al. *Materials Science & Engineering A*[J], 2006, 435-436(6): 163
- Lim H K, Son S W, Kim D H. *Journal of Alloys and Compounds*[J], 2008, 454(1-2): 515
- Mahmudi R, Moeendarbari S. *Materials Science & Engineering A*[J], 2013, 566: 30
- Liu H M, Chen Y G, Tang Y B et al. *Journal of Alloys and Compounds*[J], 2007, 440(1-2): 122
- Pekguleryuz M O. *J Jpn Inst Ligth Met*[J], 1992, 42: 679
- Duly D, Simon J P, Brechet Y. *Acta Metallurgica et Materialia*[J], 1995, 43(1): 101
- Braszczyńska-Malik K N. *Journal of Alloys & Compounds*[J], 2009, 477(1): 870
- Wu X, Yang M, Yuan F et al. *Proceedings of the National Academy of Sciences of the United States of America*[J], 2015, 112(47): 14 501

## Zn 添加对 Mg-8Al-2Sn 镁合金组织和力学性能的影响

伍华怡<sup>1</sup>, 张丁非<sup>1</sup>, 蒋璐瑶<sup>1</sup>, 冯靖凯<sup>1</sup>, 赵 阳<sup>1</sup>, 潘复生<sup>1,2</sup>

(1. 重庆大学 国家镁合金材料工程技术研究中心, 重庆 400044)

(2. 重庆市科学技术研究院, 重庆 401123)

**摘 要:** 以 Mg-8Al-2Sn 变形镁合金为研究背景, 通过在 Mg-8Al-2Sn 合金中添加 0%~2% (质量分数, 下同) 的 Zn 元素, 研究了 Zn 添加对 Mg-8Al-2Sn 挤压镁合金显微组织和性能的影响。结果表明, 铸态 Mg-8Al-2Sn-xZn 合金的相组成主要是  $\alpha$ -Mg 相、Mg<sub>17</sub>Al<sub>12</sub> 相和 Mg<sub>2</sub>Sn 相。在添加 Zn 元素以后, 合金中的共晶化合物的形态发生变化, 由共晶组织变为离异共晶组织。挤压过后, 晶粒组织尺寸更均匀。Zn 元素的加入, 会促进合金中第二相在挤压过程中的动态析出以及第二相的粗化。合金在时效中产生的析出相的数量也随着 Zn 含量的增多而增加。随着 Zn 含量的增加, 挤压态和时效态合金的屈服强度和抗拉强度都随之增加。当 Zn 含量达到 2% 时, 合金力学性能最好, 其时效态的抗拉强度, 屈服强度和延伸率分别是 385 MPa, 291 MPa 和 6.44%。

**关键词:** 镁合金; Mg-Al-Sn-Zn 挤压镁合金; 显微组织; 力学性能

---

作者简介: 伍华怡, 女, 1994 年生, 硕士, 重庆大学材料科学与工程学院, 重庆 400044, 电话: 023-65112491, E-mail: wuhuayi52@163.com